IJC Heart & Vasculature 53 (2024) 101437

Contents lists available at ScienceDirect

IJC Heart & Vasculature

journal homepage: www.sciencedirect.com/journal/ijc-heart-and-vasculature

Advanced imaging of cardiac Paraganglioma: A systematic review

Bruna Punzo [a,*], Liberatore Tramontano [a], Alberto Clemente [b], Sara Seitun [c], Erica Maffei [a], Luca Saba [d], Carlo Nicola De Cecco [e], Eduardo Bossone [f], Jagat Narula [g], Carlo Cavaliere [a], Filippo Cademartiri [b]

[a] IRCCS SYNLAB SDN, Via Emanuele Gianturco 113, Naples I-80143, Italy
[b] Department of Radiology, Fondazione Toscana Gabriele Monasterio/CNR, Pisa, Italy
[c] Department of Radiology, IRCCS Ospedale Policlinico San Martino, Genova, Italy
[d] Department of Radiology, University of Cagliari, Cagliari, Italy
[e] Division of Cardiothoracic Imaging, Department of Radiology and Imaging Sciences, Emory University Hospital-Emory Healthcare, Atlanta, GA, USA
[f] Department of Public Health, "Federico II" University of Naples, Naples, Italy
[g] Icahn School of Medicine at Mount Sinai, The Mount Sinai Hospital, New York, NY, USA

ARTICLE INFO

Keywords:
Paraganglioma
CCT
CMR

ABSTRACT

Background and aims: Cardiac ParaGangliomas (PGLs) are rare extra-adrenal tumours that arise from chromaffin cells of the sympathetic ganglia. PGL are often diagnosed incidentally, with no symptoms or symptoms related to cardiovascular dysfunction.
Methods: Cardiac Computed Tomography (CCT) and Cardiac Magnetic Resonance (CMR) can detect the correct morphology and position of the lesion and provide proper tissue characterization.
Nuclear medicine imaging, with Positron Emission Tomography (PET) or Single Photon Emission Computed Tomography (SPECT) with specific radiotracers, can evaluate the functionality of the PGL and to distinguish a secreting from a non-secreting tumour.
Results: In association with biochemical parameters, a multimodal imaging approach, not yet standardized, can be useful both in the diagnosis, in the monitoring and in the treatment planning.
Conclusions: In this systematic review, we aim to investigate the role of diagnostic imaging, in particular CCT, CMR, PET and SPECT in diagnosis, characterization and monitoring of cardiac PGLs.

1. Introduction

Rare neuroendocrine tumors known as paragangliomas (PGL) develop from neural crest cells of the parasympathetic or sympathetic ganglia outside of the adrenal gland [1]. While some of them may show symptoms of excess catecholamine because they are metabolically active, others may only be discovered accidentally [2].

In 35–50 % of instances, they are functional and are more frequently seen in the left atrium [3].

Although there are several imaging alternatives available, none seem to be the best.

This occurs because a proper diagnosis requires the association of additional information gleaned from other imaging techniques. Nuclear medicine studies like Positron Emission Tomography (PET) or Single Photon Emission Computed Tomography (SPECT) are helpful to assess the functional/metabolic activity of the tumor for the differential diagnosis. In suspected secreting or non-secreting cardiac PGL, morphological and tissue imaging examination using cardiac computed tomography (CCT) and cardiac magnetic resonance (CMR) combination with nuclear imaging is helpful.

We intend to analyze the characteristics gained through morphological imaging, such as CCT and CMR imaging, and those obtained from PET or SPECT, and how these combinations might be effective for the diagnosis, follow-up, and therapy of cardiac PGLs.

Abbreviations: PGL, ParaGangliomas; CCT, Cardiac Computed Tomography; CMR, Cardiac Magnetic Resonance; PET, Positron Emission Tomography; SPECT, Single Photon Emission Computed Tomography.

* Corresponding author.
E-mail address: bruna.punzo@synlab.it (B. Punzo).

https://doi.org/10.1016/j.ijcha.2024.101437
Received 13 March 2024; Received in revised form 27 May 2024; Accepted 29 May 2024
Available online 4 July 2024

2. Materials and methods

2.1. Clinical aspects

The clinical presentation and symptoms of cardiac paragangliomas are diverse and depend on the location of the tumor, its size, and whether it is hormonally active. Below are the primary clinical aspects and symptoms associated with cardiac paragangliomas:

Location and Origin: Cardiac PGL can occur in various parts of the heart, including the atria, ventricles, and pericardium. They originate from chromaffin cells, which are part of the sympathetic and parasympathetic nervous systems.
Imaging: Cardiac PGL are usually identified through imaging modalities such as echocardiography, CCT scans, CMR, and PET scans. CMR is particularly useful due to its superior soft tissue contrast.
Functional Status: The tumors can be classified as functional or non-functional based on their ability to secrete catecholamines. Functional tumors are more likely to present with symptoms related to catecholamine excess.

Related to the symptoms, we can distinguish cardiovascular symptoms (hypertension, palpitations, chest pain and heart failure), symptoms related to catecholamine excess such as headache, sweating, anxiety and sometimes panic attacks and other non-specific symptoms (fatigue and/or weight loss).

No less common are the phenomena of compression such as dyspnea, dysphagia and hoarseness.

The management of cardiac paragangliomas is complex and requires a multidisciplinary approach involving cardiologists, endocrinologists, oncologists, and cardiothoracic surgeons to optimize patient outcomes.

2.2. Search strategy and selection criteria

A systematic literature search was performed to identify original articles that evaluated the role of diagnostic imaging to assess cardiac PGL. The most relevant scientific electronic databases (PubMed, Scopus, Web of Science) were comprehensively explored and used to build the search. Only studies published from 2011 to 2021 were selected. The search strategy included the key terms listed in Supplementary Materials. The literature search was restricted to English language publications and studies of human subjects. Two reviewers, after having independently screened the search, identified titles and abstracts, assessed the full text of the articles describing the ability of different imaging modalities to diagnose, evaluate and characterize cardiac PGL. Review articles were excluded. For articles meeting these criteria with full text available, the following further selection criteria had to be fulfilled: articles were excluded if they also involved any type of PGL concerning other anatomical site and if they were off-topic after investigating the full text. Moreover, we only included articles demonstrating the utility of diagnostic imaging as CCT, CMR, PET and SPECT to assess and to describe cardiac PGL.

2.3. Planning and conducting the review

After the selection procedure, selected articles were analysed by two reviewers, and data useful for conducting the systematic review were collected in a predesigned sheet. Extracted data will include the following: study characteristics (first author name, publication year, type of study, number of patients, imaging methods), patient characteristics (age, diagnosis, risk factors), defined location of the PGL and its features.

This systematic review was conducted in accordance with the Preferred Reporting Items for Systematic Reviews and Meta-Analyses (PRISMA) statement [4] (PRISMA Checklist in Supplementary Materials).

2.4. Quality assessment

The quality of included studies was evaluated using the QUADAS-2 tool, by two reviewers independently, and any disagreement was resolved by consensus. According to QUADAS-2, four domains are critical for assessing biases in studies: patient selection, index test, reference standard and flow and timing. The first part of each domain concerns bias and comprises three sections: 1) information used to support the risk of bias judgment, 2) signalling questions, and 3) judgment of risk of bias by recording the information used to reach the judgment. The additional signalling questions are included to assist judgments. They are answered as “yes”, “no”, or “unclear”, and are phrased such that “yes” indicates low risk of bias. Risk of bias is judged as “low”, “high”, or “unclear”. If all signalling questions for a domain are answered “yes” then risk of bias can be judged “low”. If any signalling question is answered “no” this flags the potential for bias. The “unclear” category should be used only when insufficient data are reported to permit a judgment.

The overall quality of included studies was considered good for our purposes (Fig. 1).

3. Results

3.1. Study selection

A total of 139 articles were retrieved by scientific electronic databases search. After removal of duplicates, 127 articles were used for assessment. Considering the title and abstract, 74 records were excluded because they clearly did not match the inclusion criteria: some of these did not investigate the role of imaging in PGL, others described different lesion sites. 53 articles were evaluated on their full text. Of these, 25 records were excluded: 3 were reviews and the others were out of topic. Finally, 28 records were included for qualitative synthesis (Fig. 2).

3.2. Characteristics of included studies

The study characteristics of the 28 selected articles are described in Table 1. All selected studies were case reports on humans. For this reason, the quality assessment performed with the QUADAS-2 tool resulted in the flow and timing domain for 100 % “unclear”, given the impossibility of evaluating and/or planning patient follow-up.

Given the heterogeneity of the imaging methods used for the diagnosis and monitoring of cardiac PGL, paragraphs were furtherly subdivided to facilitate reading.

3.3. CT and PET reports

In 22 out of 28 papers, the shape, locations, and properties of the cardiac PGL were assessed using a CT scan. Only one of them, which will be detailed later, utilized CCT, CMR, PET, and SPECT.

In six of the 22 papers, the value of using PET to evaluate cardiac PGL was discussed (Fig. 3; Movie 1). The radiotracers utilized to determine the endocrine activity of the lesion and identify it as a secreting or non-secreting PGL are 18F-fluorodeoxyglucose (18F-FDG) and dopaminergic uptake radiotracers.

Gallium-68 dotatate PET was used in Chang et al. [5], which localizes neuroendocrine tumors by binding to somatostatin receptors. It was shown that there was a region of radiotracer uptake along the aortic arch. Chest CT was also conducted in order to confirm the presence of a 1.3 cm hyper-enhancing soft tissue nodule in the aortopulmonary window and to further characterize pre-operative planning, size, and placement of PGL. In **Del Forno** et al. [6], a CCT revealed an oval neoformation with uneven contrast enhancement in the right atrioventricular groove. A PET with a dopaminergic radiotracer (not adequately described) was performed since a cardiac PGL was suspected.

An instance of cardiac PGL that was missed by SPECT was described

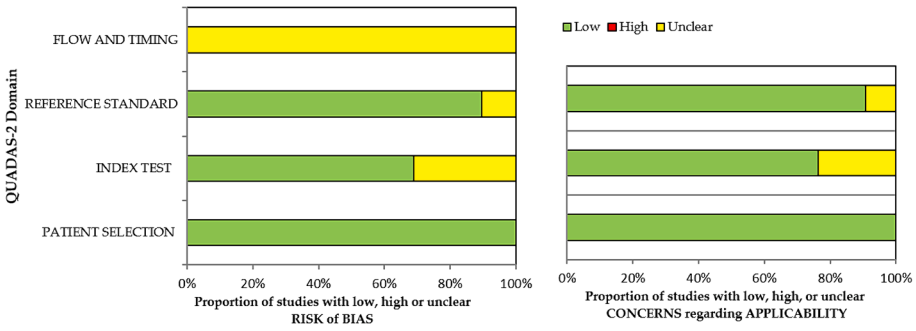

Fig. 1. Results of Quality Assessment Using Quadas Toolu.

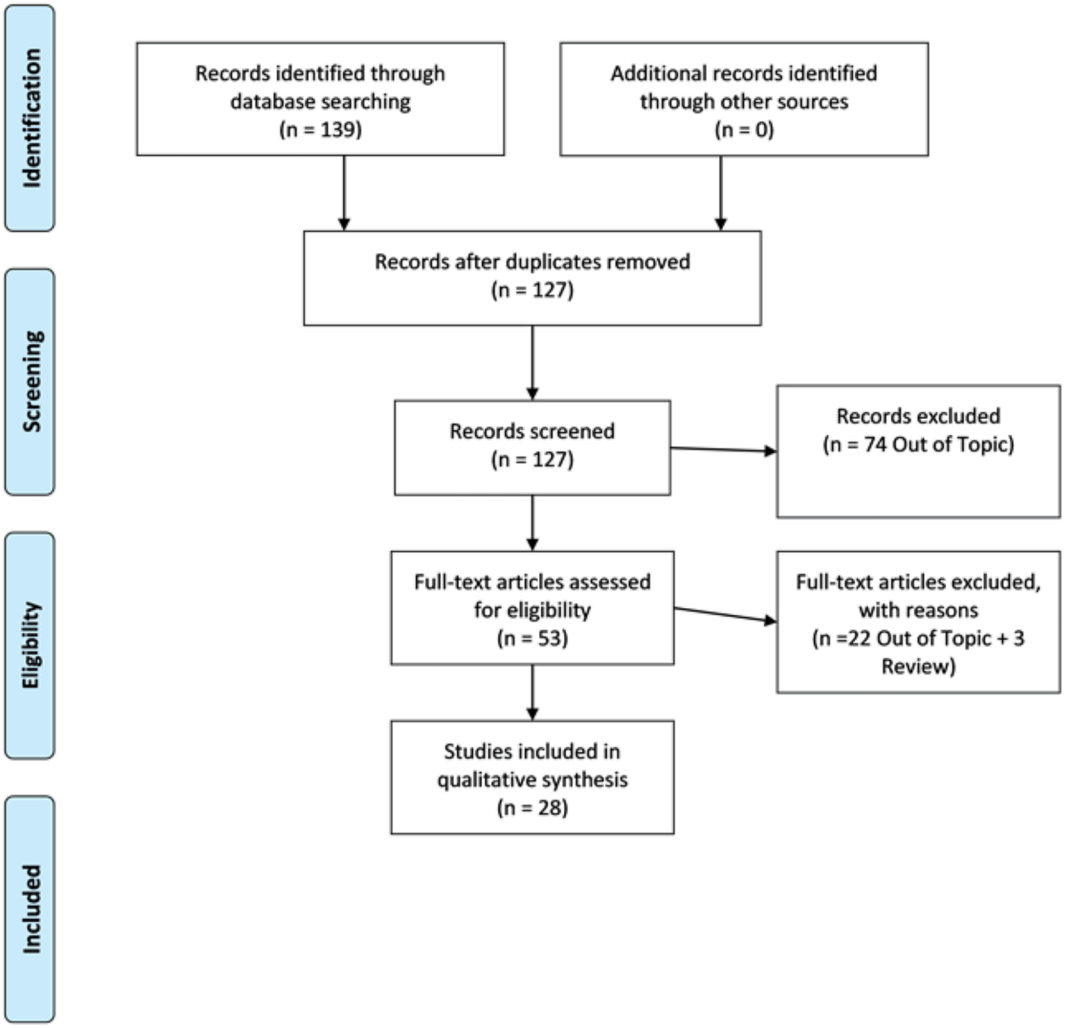

Fig. 2. PRISMA flow diagram.

by **Hinojosa et al.** [7]. Fluorine-18-L-dihydroxyphenylalanine (18F-DOPA) PET scanning emphasized the pathological finding, and a chest CT scan corroborated it by revealing a vascularized mass in the posterior mediastinum, close to the left atrium.

Another instance (**Moline et al.** [8]) had a hypermetabolic mass that emerged anterior to and extended between the aorta and the pulmonary artery/right ventricular outflow tract. This lesion was seen on the CT scan. Chest CT-angiography indicated, similarly to **Degrauwe et al.** [9], a massive, heterogeneous, and highly vascular paracardiac mass originating from the pericardium and compressing the left inferior pulmonary vein and the lateral left ventricular (LV) wall without local tissue invasion. High metabolic activity inside the paracardiac mass was detected using an 18F-FDG PET scan, ruling out the occurrence of distant metastases.

In **Bhojwani et al.** [3], a hybrid positron emission tomography/magnetic resonance imaging (PET/MRI) revealed a well-defined mass with significant contrast enhancement between the left superior pulmonary vein and pulmonary artery, where PGL seemed hypermetabolic. We will report the MRI results that the mass produced later.

The utility of accurate correlative imaging using CT and PET (e.g., with DOPA) is paramount for the detection and characterization of paragangliomas. CT scans provide high-resolution anatomical details,

Table 1
Study characteristics.

Author, Year	Number of patients	Age (years)	Gender	Study design	Risk factors	Imaging	PGL sites
Chang SH. et al. [5], 2020	1	58	M	CASE REPORT	NR	CT + PET (gallium-68 dotatate)	Aortopulmonary window
Nemeth A. et al. [1], 2020	1	21	F	CASE REPORT	Decompensated heart failure, sub-febrile temperature, head and joint pain, and nonproductive cough.	CT	Top of the left atrium
Hai Z. et al [10], 2018	1	22	F	CASE REPORT	Hypertension,palpitation, headache, and excessive sweating.	CTCA + OCTREOSCAN	Right atrioventricular groove
Alraddadi HO. et al. [14], 2018	1	29	M	CASE REPORT	Persistentanxiety, dyspnea, palpitations, and headaches/FE 33 %.	CT + MIBG	RVOT
Fan J. et al. [19], 2018	1	39	M	CASE REPORT	Nocturnal intermittent palpitation.	CMR + PET	Right atrium
Berona K. et al. [16], 2018	1	34	F	CASE REPORT	Palpitations and shortnessof breath/blood pressure was noted to be 159/80 mm Hg.	CT + CMR + MIBG	posterolateralto the left atrium
Saththasivam P. et al. [28], 2017	1	57	F	CASE REPORT	Hypertension,anxiety.	CMR	Intrapericardialmass/ aorticopulmonary
Tam DY et al. [11], 2017	1	25	F	CASE REPORT	Anemia, anxiety, palpitations.	CT + OCTREOSCAN	Atrioventricular groove
Gahremanpour A. et al. [23], 2017	1	24	F	CASE REPORT	Episodic hypertension and palpitation.	CMR + MIBG	Left atrial roof
Degrauwe S. et al. [9], 2017	1	43	M	CASE REPORT	NR	CTA + CMR + PET FDG	Basal lateral leftventricular
Almenieir N. et al. [30], 2017	1	25	F	CASE REPORT	Palpitations.	CT + CMR + MIBG + PET FDG	Right atrioventriculargroove
Hinojosa CA. et al. [7], 2017	1	21	F	CASE REPORT	Progressive and uncontrolled arterial hypertension.	CT + PET F-DOPA	Retrocardiac
Romano S. et al. [18], 2017	1	28	M	CASE REPORT	Intermittent palpitations, dyspnoea and anxiety.	CT + CMR + MIBG	Behind the left atrium
Bhojwani N. et al. [3], 2017	1	42	M	CASE REPORT	Left-sided chest pain, smoking, atrial fibrillation,hypertension, and hyperlipidemia.	CTA + CMR + PET	Between the left superior pulmonary vein and pulmonary artery, above the left anterior descendingartery
Marchand L. et al. [29], 2016	1	75	F	CASE REPORT	NR	MIBG + PET FDG	Retrocardiac
Del Forno B. et al. [6], 2016	1	46	F	CASE REPORT	Intermittent hypertension,palpitation, and familiarity with vertebral paraganglioma.	CTA + CMR + PET DOPA	Right atrioventricular groove
Gonzalez-Santos JM. et al. [12], 2016	1	60	M	CASE REPORT	NR	CT + OCTREOSCAN	Aortopulmonarywindow
Yadav PK. et al. [2], 2014	1	73	F	CASE REPORT	NR	CMR	Above the left atrium
El-Ashry AA. et al. [24], 2014	2	34	M	CASE REPORT	1) Hypertension, chest pain, paroxysmalpalpitations, sweating, and anxiety 2) Severe hypertension and elevated vanillylmandelic acid level.	1) MR 2) CT	1) Left atrial wall 2) Right atrial wall
Millar AC. et al. [15], 2014	1	41	M	CASE REPORT	Family history for coronary artery disease.	CTA + CMR + SPECT	Right atrium and left atrium roof
Ojiaku M. et al. [26], 2014	1	38	M	CASE REPORT	History of night sweats, nonproductive cough, and weight loss.	CTA + CMR	Adjacent to the aortic root
Xia HM. et al. [25], 013	1	49	F	CASE REPORT	Short breath after activity and atypical chest discomfort.	CT	Intrapericardial massin the left atrium
Ghouri MA. et al. [27], 2013	1	81	M	CASE REPORT	Neck pain and dyspnea, hypertension, intermittent palpitations and anxiety.	CT	Aortopulmonarywindow
Liu X. et al. [13], 2013	1	47	F	CASE REPORT	Longstandinghypertension.	CT + MIBG	Interatrial groove
Beroukhim RS. et al. [22], 2012	1	16	M	CASE REPORT	Irregular heart rhythm.	CT + CMR	Aortopulmonarywindow
Moline J. et al. [8], 2011	1	62	M	CASE REPORT	Prostate cancer, diabetes, hyperlipidaemia aandcough.	CT + PET FDG	RVOT
Corsello SM. et al. [17], 2011	1	41	F	CASE REPORT	Hypertensive crises associated with headache, sweating,and tachycardia	CT + CMR + MIBG	Left superior pulmonary vein
Duan YH. et al. [20], 2011	1	22	F	CASE REPORT	Palpitation and hypertension after adrenalectomy	CMR + PET FDG	On the top of the left atrium

Abbreviations: Cardiac Magnetic Resonance (**CMR**); Computed Tomography (**CT**); Computed Tomography Angiography (**CTA**); Computed Tomography Coronary Angiography (**CTCA**); Iodine-131-meta-iodobenzylguanidine (**MIBG**); Magnetic Resonance (**MR**); Positron Emission Tomography (**PET**); Paraganglioma (**PGL**); Right Ventricular Outflow Tract (**RVOT**); Single Photon Emission Tomography (**SPECT**).

while PET imaging, particularly with radiotracers such as 18F-DOPA, offers functional insights by highlighting areas of increased metabolic activity. This combined imaging approach significantly enhances the ability to precisely locate the tumor, assess its size, and understand its metabolic profile, which is crucial for effective diagnosis and treatment planning.

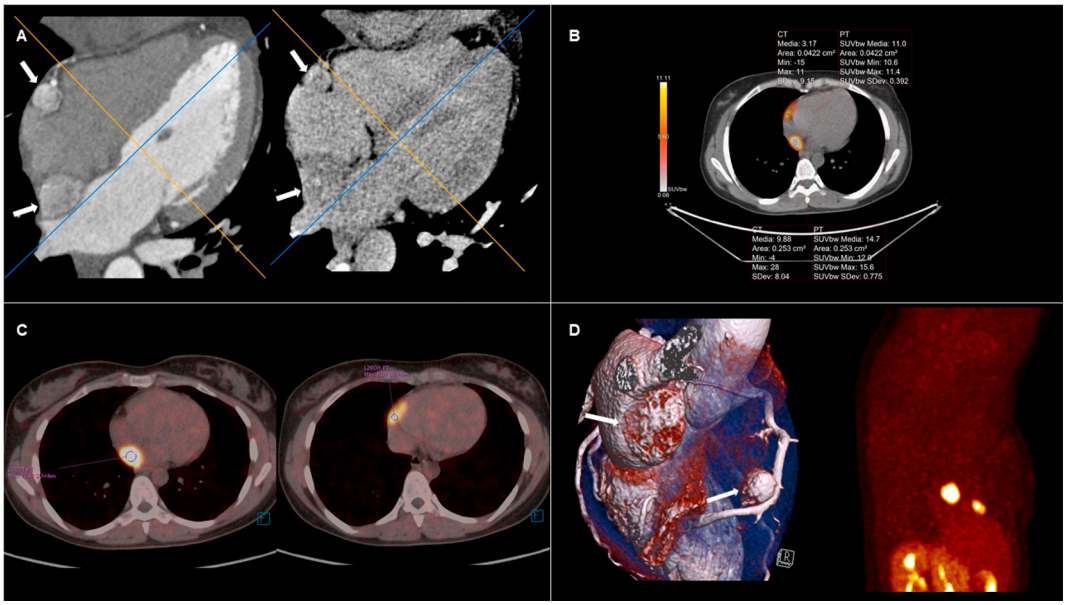

Fig. 3. Example of Multimodality Imaging of a Multiple Paraganglioma of Heart; Part I. A) Cardiac CT in early (on the left) and late post-contrast acquisition (on the right) showing two cardiac PGLs (white arrows); B and C) Fused PET-CT (F-Dopa) images with hyper-metabolic PGLs (SUV values reported for each lesion); D) Cinematic rendering CT reconstruction (white arrows for PGLs); E) oblique sagittal PET reconstruction (white arrows for PGLs). See Movie 1.

3.4. CCT and SPECT reports

Nine of the 22 articles, used CT imaging combined with traditional nuclear medicine imaging such as SPECT.

When PGL was suspected, in association with CT morphologic assessment, SPECT with Indium In-111 pentetreotide (Octreoscan) can be performed to diagnose neuroendocrin origin.

The method uses a somatostatin analogue labeled with In 111 and recognizing somatostatin receptors on the cell surface of these tumors, allowing to identify neoplastic agglomerates. The method also allows a prognostic evaluation in relation to the receptor density in vivo, allowing to consider the analogues themselves for therapy.

Hai et al. [10], **Tam et al.** [11] and **Gonzalez et al.** [12] treated cases of PGL which have performed CT scans and SPECT with octreotide radiotracer.

A strong localized uptake around the right heart was seen in Hai et al. The tumor was visible projecting into the right atrium when somatostatin receptor scintigraphy and CT images were registered together. An octreotide scan with Indium-111 performed by Tam et al. and Gonzalez et al. revealed a localized uptake for the cardiac mass. In a different instance, **Liu et al.** [13] showed mediastinum-specific 99mTc-labelled octreotide focal uptake. A spherical solid mass that extended anteriorly and posteriorly down the right side of both atria and covered the interatrial groove was visible on a CT scan.

Iodine-131-meta-iodobenzylguanidine was the radiotracer utilized in the other 5 papers to conduct SPECT scans (MIBG). In **Alraddadi et al.** [14], a 123I-MIBG corroborated a CT scan finding of a mediastinal mass between the aortic root and the pulmonary artery. Similar to this, a SPECT with MIBG performed by **Millar et al.** [15] revealed that the mediastinal bulk avidly absorbed the tracer whereas other locations did not. CT scans of the abdomen and pelvis revealed no further signs of metastases.

A mildly mass-effecting posterolateral mass to the left atrium was detected by CT pulmonary angiography in **Berona et al.** [16] and later verified by a 123I-MIBG scan.

Cardiovascular PGL was identified in **Corsello et al.** [17] and **Romano et al.** [18] by integrating several radiological and nuclear medicine methods (such as SPECT with 123I-MIBG scan, chest CT, and CMR). Chest CT revealed a confined subcarinal mass behind the left atrium, and 123I-MIBG indicated a single focused uptake in the mediastium.

3.5. CMR and PET reports

16 of 28 articles used CMR as imaging method to diagnose PGL. 5 of these 16 articles, described the usefulness of the PET in association with CMR to assess and confirm the presence of cardiac PGL (Fig. 4; Movie 1).

A synchronized CCT scan performed by **Del Forno et al** [6] revealed an oval neoformation with inhomogeneous contrast enhancement in the right atrioventricular groove. A spherical mass in the right atrioventricular groove was visible on an integrative CMR scan, although the heart chambers did not appear to have been invaded. The lesion was T1 hypointense heterogeneous, mildly hyperintense on T2, and significantly hyperintense in sequences that suppress fat. When a dopaminergic radiotracer was used during a PET, the lesion substantially uptake.

According to **Fan et al.** [19], an individual with elevated blood catecholamine metabolites had a CMR instance of cardiac PGL that was later validated by PET.

According to **Degrauwe et al.** [9], CMR imaging revealed a sizable, distinct, and well-circumscribed intrapericardial mass that was at the level of the basal LV lateral wall and extended toward the atrioventricular groove. With no hyper-captation of distant organs and significant metabolic activity inside the paracardiac mass, 18F-FDG PET ruled out the occurrence of metastases.

A sizable tumor on the top of the left atrium was described by **Duan et al.** [20] with 18F-FDG PET hyper-metabolism but no metastatic lesions. The SDHB (Succinate dehydrogenase B subunit) mutations, associated with increased malignant potential, may be the cause of enhanced 18F-FDG uptake [21]. The mass was better characterized using CMR, which revealed a sizable, well-circumscribed, ovoid-shaped mass next to the left atria that was heterogeneously hyperintense on T1 imaging and hyperintense on T2 imaging, typical PGL results.

With no distant metastases identified by 18F-FDG PET in **Beroukhim et al.** [22], the CMR sequences were consistent with a robust vascular supply to the tumor.

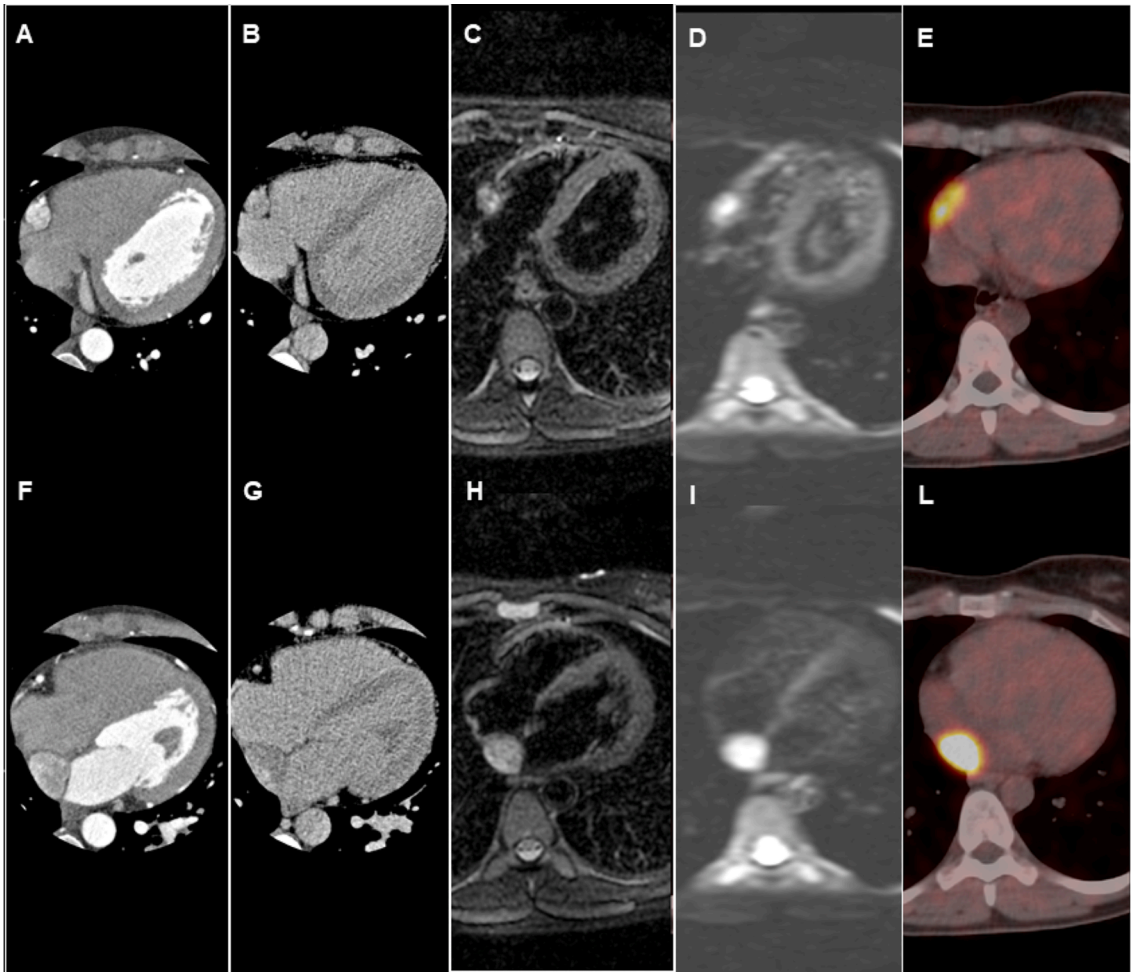

Fig. 4. Example of Multimodality Imaging of a Multiple Paraganglioma of Heart; Part II. Multimodal imaging of two cardiac PGLs sited along the right atrioventricular sulcus (A, B, C, D, E) and interatrial groove (F, G, H, I, L). From the left side: axial cardiac CT (A, F for early post-contrast acquisition; B, G for late post-contrast acquisition); axial four-chamber cardiac MR withT2-weighted (C, H) and diffusion-weighted (D, I) sequences; fused PET-CT (F-Dopa) image (E, L). See Movie 1.

3.6. CMR and SPECT reports

5 of 16 articles used CMR imaging combined with traditional nuclear medicine imaging such as SPECT. In all these reports, the radiotracer used to characterize PGL was MIBG

A SPECT with MIBG in the instance of **Gahremanpour et al.** [23] revealed high tracer absorption only in the subcarinal region. The posterior left atrium wall of the patient had a non-moving, well-circumscribed mass, which was detected by a T1-weighted echo inversion-recovery CMR sequence. On T1- and T2-weighted images, the mass displayed a strong signal intensity and significant contrast enhancement. Similarly, in **Millar et al.** [15], the mass was significantly hyperintense on T2-weighted imaging and was somewhat hyperintense in relation to the thoracic muscles, which is a symptom frequently found in PGL.

In **Berona et al.** [16], CMR exhibited a modest mass impact upon the left atrium and left pulmonary vein in addition to a T1 and T2 hyperintense ovoid mass in the posterolateral to the left atrium. A MIBG scan confirmed increased uptake in the left perihilar region, compatible with a tumour of neural crest origin.

Similar to **Romano et al.** [18], **Corsello et al.** [17] presented a case of retrocardiac PGL that was identified by MIBG scan and exhibited a single localized uptake in the mediastium. The CT scan revealed a subcarinal retrocardiac mass that was compressing the left atrium and exhibiting nonhomogeneous enhancement with hypodense regions near to the left superior pulmonary vein. CMR imaging supported the diagnosis.

3.7. CT and/or CMR reports

Only 7 articles did not use nuclear medicine imaging such as PET or SPECT. The morphological evaluation is performed with CT or CMR scans.

Two instances were mentioned in **El-Ashry et al.** [24] study using CT and CMR acquisitions. By concentrating on resection surgery, this article only briefly discussed the function of diagnostics.

A tumor in the middle mediastinum was discovered by chest CT angiography in **Xia et al.** [25]. The surgical removal by extracorporeal circulation was planned and carried out successfully based on the transesophageal echocardiography results of an encapsulated tumour without surrounding invasion.

A cardiac mass was found on top of the left atrium with contact to the pulmonary trunk, ascending aorta, and left ventricle (LV) in **Nemeth et al.** [1] CT scan.

In **Ojiaku et al.** [26], CCT showed a significant heterogeneous, highly enhancing mass within the left ascending aorta, anterior to the left atrium, and slightly above the anterior wall of the left ventricle. The left paraaortic area was found by CMR to have a sizable, well-circumscribed mass emerging from the pericardium. On T1-weighted pictures, the mass was isointense to the myocardium, and on T2-

weighted images, it was substantially hyperintense. A multi-lobular, high-density lesion between the aorta and the pulmonary artery was found on CT in the research of **Ghouri et al.** [27] just like in Ojiaku et al. Clinicians evaluated the patient's 24-hour urine vanillylmandelic acid levels because they suspected PGL. These weren't increased, which indicated that the PGL wasn't working.

CMR was used in the instance of **Yadav et al.** [2] to more thoroughly assess cardiac PGL since it revealed a highly vascularized lesion that was perhaps a haemangioma, angiosarcoma, or PGL.

Angiosarcomas present as irregular, invasive, low-attenuating nodular masses, whereas haemangiomas often exhibited intermediate intensity on T1 and hyperintensity on T2. Cardiac PGLs are frequently observed, as in this patient, on the roof of the left atrium and are generally hyperintense on T2 imaging. Instead, CMR imaging was used to further define a mass that was encasing the right and left coronary arteries, the aortic root, and the pulmonary artery trunk in **Saththasivam et al.** [28]. On the basis of imaging and biochemical studies, the levels of urine-metanephrine, nor-metanephrine, and vanillyl-mandelic acid were all within the normal range, pointing to a diagnosis of non-functional PGL.

3.8. PET and SPECT reports

Only one of 28 articles selected, described PGL finding through only nuclear imaging acquisitions. According to **Marchand et al.** [29], the retrocardiac lesion on 18F-FDG PET scan was hypermetabolic and had a noticeably enhanced uptake on SPECT with MIBG. This led to the lesion being labeled as a functional PGL.

3.9. Reports using CT, CMR, PET and SPECT

Only one of 28 articles selected showed the evaluation of the PGL through all the methods mentioned. Chest CT and CMR were used to perform morphological evaluation in **Almenieir et al.** [30]. A cardiac haemangioma was suggested by the imaging features of the mass, which were revealed by CT to be heterogeneously hyper-enhancing with a core stellate "scar" focused on the right atrium. Cardiac PGL was one of the possible diagnoses. The lesion was not otherwise characterized by the CMR scan, which revealed that it was mostly solid with a few tiny cystic components. SPECT with MIBG was used to better assess functional behavior and treatment alternatives, and the results revealed only a minor heterogeneous buildup of radiotracer in the bulk. To exclude metastases, 18F-FDG PET was used. It revealed that the mass had severe core necrosis and strong hypermetabolism.

4. Discussion

Chromaffin tumors called PGLs develop from neural crest cells. Only around 2 % of PGLs, or 10 % of all PGLs, are cardiac PGLs, which are generally seen in the posterior mediastinum of the chest [1].

The most frequent site of origin was the left atrium, which accounted for 38.5 % of all cases, followed by the right atrium (19.2 %), aorto-pulmonary window (18 %), left ventricle (7.7 %), atrioventricular groove (6.4 %), inter-atrial septum (5.1 %), and right ventricle (4 %), according to research [31].

PGL are normally benign, but 10 % of cases may be malignant with local invasion of the pericardium and conduction system [32] and distant metastases. Additionally, it is difficult to distinguish between benign and malignant cardiac PGL due to a lack of evidence and histopathological criteria. The preferred form of treatment is surgical resection.

CT imaging might show that the tumor was initially localized to the middle mediastinum. In fact, 78,6 % of the papers mentioned making the first diagnosis using a heart or chest CT scan. This technique works extremely well to pinpoint the lesion's precise location, degree of vascularization, and shape. In contrast to a chest CT, a cardiac CT may eliminate heartbeat artifacts by triggered acquisitions, and the retrospective approach enables data sets to be reconstructed in various planes and cardiac cycle phases.

CMR is helpful in the diagnosis and monitoring of cardiac mass for the morphological evaluation. As a result of this inquiry, the lesion's location and its connection to the nearby structures may be determined by the analysis of the cardiac planes. The morphological characteristics of hyper/hypointensity are suitable to discriminate the lesion and the relationship with the other structures are much better highlighted.

For a more thorough analysis of these masses, CT and CMR are both helpful. Differentiating between pericardial masses can be aided by attenuation on CT scans, tissue characterisation on CMR scans, patterns and intensities of contrast enhancement, and the presence or absence of blood flow on cine CMR pictures. The first pass post-contrast imaging's brisk perfusion implies a tumor with abundant vascular supply, further reducing the differential diagnosis to haemangioma, angiosarcoma, or PGL.

The majority of cardiac PGL have significant T2 weighted signals, which can distinguish tumors from nearby circulatory tissues. Blood flow within the tumor prevents signals from being sent [33]. PGLs are often seen on the left atrium's roof [2]. CMR appears to be especially helpful in tumors adjacent to the heart or to the major arteries since it can characterize soft tissue to some extent [32].

In 42.8 % of the papers analyzed, nuclear imaging in conjunction with CCT and/or CMR has proven to be helpful.

In challenging circumstances, extra-adrenal PGL and metastases can be localized by SPECT and MIBG. Sadly, 10 % of PGLs are false negatives, and false positive pictures are quite uncommon. Malignant lesions have a nearly 100 % specificity rate [33]. Malignant PGLs exhibit local invasion or pericardial effusion development. To distinguish between benign and malignant cardiac PGL, there is currently little data and histopathological criteria [1].

Instead, in around 70 % of instances, octreotide scanning can photograph the PGL. A small percentage of patients who had negative MIBG scan results can have positive octreotide scan results.

Right now, PET techniques that use radiotracers that bind to somatostatin receptors are more accurate than octreoscan scintigraphy.

PET is carried out using 18F-FDG in addition to certain radiotracers. The assessment of PGLs has a significant function for the PET scan [34].

Only 36 % of the patients in our study were evaluated using PET. Functional imaging is helpful in identifying PGL with unclear localisation and/or in the detection of additional lesions, hence PET acquisition in conjunction with CT or MR imaging can be crucial in the assessment of both the main tumor and distant metastases.

5. Conclusions

This systematic review shows the ability of a multimodal morphological imaging approach obtained with CCT and CMR, combined with nuclear imaging (PET and SPECT), to correctly identify, locate and characterize cardiac paragangliomas.

Funding

This work was partially funded by the Italian Ministry of Health: "ricerca corrente" and "RCR-2019-23669118_005 CARDIO - Carditox-CT study" projects.

CRediT authorship contribution statement

Bruna Punzo: Writing – original draft, Methodology, Data curation, Conceptualization. **Liberatore Tramontano:** Formal analysis. **Alberto Clemente:** Supervision. **Sara Seitun:** Supervision. **Erica Maffei:** Visualization. **Luca Saba:** Visualization. **Carlo Nicola De Cecco:** Validation. **Eduardo Bossone:** Supervision. **Jagat Narul:** Supervision. **Carlo Cavaliere:** Validation. **Filippo Cademartiri:** Visualization, Validation.

Declaration of competing interest

The authors declare that they have no known competing financial interests or personal relationships that could have appeared to influence the work reported in this paper.

Acknowledgements

CNDC received research grant support from Siemens Healthineers.

Appendix A. Supplementary data

Supplementary data to this article can be found online at https://doi.org/10.1016/j.ijcha.2024.101437.

References

[1] A. Nemeth, C. Schlensak, A. Popov, Extended resection of a cardiac paraganglioma-A rare neuroendocrine manifestation of the heart, J. Card. Surg. 35 (3) (2020) 700–702, https://doi.org/10.1111/jocs.14440.
[2] P.K. Yadav, G.A. Baquero, J. Malysz, et al., Cardiac paraganglioma, Circ. Cardiovasc. Interv. 7 (6) (2014) 851–856, https://doi.org/10.1161/CIRCINTERVENTIONS.114.001856.
[3] N. Bhojwani, J. Huang, V. Garg, et al., Utility of ^{18}F-fluorodeoxyglucose positron emission tomography/magnetic resonance imaging in the diagnosis of cardiac paraganglioma, Indian J. Nucl. Med. 32 (4) (2017) 380–382, https://doi.org/10.4103/ijnm.IJNM_93_17.
[4] D. Moher, A. Liberati, J. Tetzlaff, D.G. Altman, PRISMA Group. Preferred reporting items for systematic reviews and meta-analyses: the PRISMA statement, PLoS Med. 6 (7) (2009) e1000097, https://doi.org/10.1371/journal.pmed.1000097.
[5] S.H. Chang, I. Yapar, B.D. Kozower, Aorticopulmonary Paraganglioma with symptomatic postoperative bradycardia, Ann. Thorac. Surg. 109 (5) (2020) e367–e369, https://doi.org/10.1016/j.athoracsur.2019.08.046.
[6] B. Del Forno, C. Zingaro, E. Di Palma, et al., Cardiac paraganglioma arising from the right atrioventricular groove in a paraganglioma-pheochromocytoma family syndrome with evidence of SDHB gene Mutation: an Unusual Presentation, Ann. Thorac. Surg. 102 (3) (2016) e215–e216, https://doi.org/10.1016/j.athoracsur.2016.01.072.
[7] C.A. Hinojosa, H. Laparra-Escareno, J.E. Anaya-Ayala, et al., Right thoracoabdominal approach for retrocardiac paraganglioma resection, Tex. Heart Inst. J. 44 (1) (2017) 62–65, https://doi.org/10.14503/THIJ-15-5561.
[8] J. Moline, J. Ngeow, P. Rajiah, C. Eng, Evil lurks in the heart of man: cardiac paraganglioma presenting as recurrent dyspnoea and chronic cough, bcr1120115170, BMJ Case Rep. (2011), https://doi.org/10.1136/bcr.11.2011.5170.
[9] S. Degrauwe, P. Monney, S.D. Qanadli, et al., Intrapericardial paraganglioma: the role of integrated advanced multi-modality cardiac imaging for the assessment and management of rare primary cardiac tumors, Cardiol. J. 24 (4) (2017) 447–449, https://doi.org/10.5603/CJ.2017.0091.
[10] Z. Hai, S. Guangrui, Cardiac paraganglioma, Eur. Heart J. 39 (23) (2018) 2219, https://doi.org/10.1093/eurheartj/ehu241.
[11] D.Y. Tam, R.J. Cusimano, Cardiac paraganglioma, CMAJ 189 (30) (2017) E996, https://doi.org/10.1503/cmaj.170067.
[12] J.M. González-Santos, M.E. Arnáiz-García, Á. Muñoz-Herrera, J. López-Rodríguez, Mediastinal paraganglioma fed by the left circumflex artery, Interact. Cardiovasc. Thorac. Surg. 23 (5) (2016) 835–836, https://doi.org/10.1093/icvts/ivw197.
[13] X. Liu, Q. Miao, H. Zhang, et al., Primary cardiac pheochromocytoma involving both right and left atria, Ann. Thorac. Surg. 95 (1) (2013) 337–340, https://doi.org/10.1016/j.athoracsur.2012.05.084.
[14] H.O. Alraddadi, A. Alsagheir, E.P. Belley-Côté, et al., Cardiac pheochromocytoma encasing the left main coronary artery, J. Card. Surg. 33 (4) (2018) 176–178, https://doi.org/10.1111/jocs.13560.
[15] A.C. Millar, O. Mete, R.J. Cusimano, et al., Functional cardiac paraganglioma associated with a rare SDHC mutation, Endocr. Pathol. 25 (3) (2014) 315–320, https://doi.org/10.1007/s12022-013-9296-1.
[16] K. Berona, R. Joshi, Y.J. Woo, J. Shrager, Postpartum diagnosis of cardiac paraganglioma: a case report, J. Emerg. Med. 55 (4) (2018) e101–e105, https://doi.org/10.1016/j.jemermed.2018.05.034.
[17] S.M. Corsello, R.M. Paragliola, P. Locantore, et al., Retrocardiac catecholamine-producing paraganglioma, J. Clin. Endocrinol. Metab. 96 (9) (2011) 2663–2664, https://doi.org/10.1210/jc.2011-0444.
[18] S. Romano, C. Fava, P. Minuz, A. Farzaneh-Far, Succinate dehydrogenase gene mutation with cardiac paraganglioma: multimodality imaging and pathological correlation, Eur. Heart J. 38 (23) (2017) 1853–1854, https://doi.org/10.1093/eurheartj/ehx007.
[19] J. Fan, Z. Wu, Y. Kang, Functional paraganglioma in the right atrium, Anatol. J. CardiOl. 19 (2) (2018) E2, https://doi.org/10.14744/AnatolJCardiol.2017.8241.
[20] Y. Duan, R. Xu, W. Liu, et al., PET/CT in a patient with cardiac paraganglioma, Int. J. Cardiovasc. Imaging 37 (4) (2021) 1473–1477, https://doi.org/10.1007/s10554-020-02101-2.
[21] B.A. Guenthart, W. Trope, W. Keeyapaj, et al., Intracardiac paragangliomas: surgical approach and perioperative management, Gen. Thorac. Cardiovasc. Surg. 69 (3) (2020) 555–559, https://doi.org/10.1007/s11748-020-01503-2.
[22] R.S. Beroukhim, P. del Nido, L.A. Teot, K. Janeway, T. Geva, Cardiac paraganglioma in an adolescent, Circulation 125 (5) (2012) e322–e324, https://doi.org/10.1161/CIRCULATIONAHA.111.043968.
[23] A. Gahremanpour, G. Pattakos, R.M. Reul, M. Mirzai-Tehrane, Diagnostic imaging and treatment of a left atrial paraganglioma, Tex. Heart Inst. J. 44 (4) (2017) 296–298, https://doi.org/10.14503/THIJ-16-5749.
[24] A.A. El-Ashry, R.J. Cerfolio, S.P. Singh, D. McGiffin, Cardiac paraganglioma, J. Card. Surg. 30 (2) (2015) 135–139, https://doi.org/10.1111/jocs.12479.
[25] H.M. Xia, Y. Jiang, Cardiac paraganglioma, J. Am. Coll. Cardiol. 61 (18) (2013) e167, https://doi.org/10.1016/j.jacc.2012.10.061.
[26] M. Ojiaku, E. Peña, E.C. Belanger, K.L. Chan, C. Dennie, Functioning intrapericardial paraganglioma: multimodality imaging findings and pathological correlation, Circulation 130 (16) (2014) e137–e139, https://doi.org/10.1161/CIRCULATIONAHA.114.012458.
[27] M.A. Ghouri, E. Krishnan, A. Singh, T. Zaman, C.H. Hallman, Mediastinal paraganglioma between the great vessels in an 81-year-old woman, Tex. Heart Inst. J. 40 (2) (2013) 189–192.
[28] P. Saththasivam, E. Herrera, O.A. Jabbari, M. Reardon, R. Sheinbaum, Cardiac paraganglioma resection with ensuing left main coronary artery compromise, J. Cardiothorac. Vasc. Anesth. 31 (1) (2017) 236–239, https://doi.org/10.1053/j.jvca.2016.05.048.
[29] L. Marchand, L. Garby, C. Nozières, G. Raverot, F. Borson-Chazot, An old retrocardiac mass fortuitously reclassified as paraganglioma, Ann. Endocrinol. (Paris) 77 (6) (2016) 668–669, https://doi.org/10.1016/j.ando.2016.06.002.
[30] N. Almenieir, S. Karls, V. Derbekyan, R. Lisbona, Nuclear Imaging of a Cardiac Paraganglioma, J. Nucl. Med. Technol. 45 (3) (2017) 247–248, https://doi.org/10.2967/jnmt.116.182212.
[31] M.F. Khan, S. Datta, M.M. Chisti, M.R. Movahed, Cardiac paraganglioma: clinical presentation, diagnostic approach and factors affecting short and long-term outcomes, Int. J. Cardiol. 166 (2) (2013) 315–320, https://doi.org/10.1016/j.ijcard.2012.04.158.
[32] M.L. Brown, G.E. Zayas, M.D. Abel, W.F. Young Jr, H.V. Schaff, Mediastinal paragangliomas: the mayo clinic experience, Ann. Thorac. Surg. 86 (3) (2008) 946–951, https://doi.org/10.1016/j.athoracsur.2008.04.105.
[33] M. Sook, E. Hamoir, L. de Leval, et al., Cardiac paraganglioma: diagnostic work up and review of the literature, Acta Chir. Belg. 112 (4) (2012) 310–313.
[34] J.W. Lenders, Q.Y. Duh, G. Eisenhofer, et al., Endocrine Society. Pheochromocytoma and paraganglioma: an endocrine society clinical practice guideline, J. Clin. Endocrinol. Metab. 99 (6) (2014) 1915–1942, https://doi.org/10.1210/jc.2014-1498.